Performance of Mild Steel and Corrosion-Resistant Steel Rebars in Chloride-Contaminated Concrete

Muazzam Ghous Sohail
Associate Professor, Department of Civil Engineering, Capital University of Science and Technology, Islamabad, Pakistan
Muazzam.sohail@cust.edu.pk

Nasser Al Nuaimi
AVP Research & Graduate Studies/ Associate Professor Department of Civil Engineering, Qatar University, Doha, Qatar
anasser@qu.edu.qa

Wael Alnahhal
Associate Professor, Department of Civil and Architecture Engineering, College of Engineering, Qatar University, Doha, Qatar

Ramazan Kahraman
Professor, Department of Chemical Engineering, College of Engineering, Qatar University, Doha, Qatar
ramazank@qu.edu.qa

Abstract

Reinforced concrete (RC) infrastructure in Arabian Peninsula is subjected to harsh climatic conditions of high temperatures, humidity, and airborne chlorides and there is a high concentration of salts in seawater and soils. These factors instigate corrosion of reinforcing steel in RC infrastructure at the early stages of the service life. To overcome the durability issues of RC infrastructures, corrosion-resistant reinforcing bars are employed. In this study, a comparison of microcell and macrocell corrosion of mild steel (MS) and two types of corrosion-resistant rebar namely the high chromium (HC) and stainless steel (SS) was established. Nine concrete block samples of $20 \times 10 \times 350$ mm were cast with top rows of reinforcements, the top row consists of MS, HC, or SS, and the bottom row contained only SS. Blocks were conditioned under 3.5% NaCl for 2 years and linear polarization resistance and macrocell currents were evaluated to compare the corrosion performance of mild and corrosion resistant steel rebars. It was observed that SS is the most corrosion-resistant steel rebar, where high chromium steel showed up to three times more corrosion resistance than mild steel under chloride attack.

Keywords: Corrosion of steel in concrete; High chromium steel; Stainless steel; Macrocell corrosion durability of reinforced concrete

1 Introduction

Chloride-induced corrosion is the major cause of concrete infrastructure deterioration. Corrosion causes spalling and cracking of concrete cover, which in turn reduces the serviceability of the structures. The repair cost to corrosion-damaged infrastructures is up to 3.5% of GDP in the US and up to 5% in the middle eastern region. Furthermore, the reduced service life of RC infrastructure has become a major burden on the economy (Al Hashem, 2011; Lim, 2012).

Concrete is inherently porous and allows several ionic species to diffuse or penetrate up to the steel surface. These ions, such as chlorides, CO2, and other gases cause the corrosion of steel. Even high-performance concrete is prone to cracking (Sohail et al., 2018b, 2020b). That is why the rebars need to be corrosion-resistant under harsh climatic conditions (Ghous Sohail et al., 2022; Sohail et al., 2018a).

Stainless steel (SS) and high chromium (HC) steel are the two main candidates for this purpose. The SS has chromium contents of up to 18% while the HC has up to 9%. These additions reduce the corroding tendency of these two types of steel compared to mild steel. Mild steel has chromium from 0 to 1% max (Mohamed et al., 2013; Team, 2007; Sohail et al., 2019).

Several researchers have evaluated the corrosion performance of SS and HC in comparison to MS. The manufacturers of HC have suggested that its performance in resisting corrosion is similar to SS. However, other researchers have shown that its corrosion is up to 2-3 times higher than MS and several levels less than stainless steel (Cui & Krauss, 2008; Nachiappan & Cho, 2005; Sohail et al., 2020a, 2021). Fahim et al. (2019) tested in corrosion performance of MS, HC, 316 LN SS, 304 SS, and XM 28 SS in concrete pore solution, in cracked and uncracked concrete. The composition of steel rebar played a significant role in the chloride threshold values that initiate corrosion, the passive layer formation, and the corrosion rates. Sohail et al. (2020) observed that the corrosion resistance of HC is two times higher than MS under a chloride solution.

In this study, the corrosion performance of mild steel, high chromium steel and stainless was evaluated while under chloride attack. The acceleration was carried out in such a way that it matches the natural corrosion of steel in concrete. The southern exposure tests were applied on the concrete block samples, which comprised wetting and drying for two years under 3.5% NaCl solution. The geometry of block samples and reinforcement placement was also kept in such a way that it simulates the real condition in RC structures. The results of this study will help engineers and designers select the reinforcement type for the conditions encountered in the field. Especially in locations where corrosion due to chloride is a durability concern.

2 Experimental Detail

Three concrete block samples of 20 × 10 × 30 cm were cast; the mold is shown in **Fig. 1**. Two reinforcement rows were fixed in the mold. The top was the bars to be studied while at the bottom for the reference to measure the macrocell corrosion were the stainless steels. Each bar was connected to an electric wire for electrochemical measurements. The length of each rebar was 30 cm and the diameter of 16 mm.

Fig. 1: Mold for block samples with a top row with either mild steel/high chromium/stainless steel, and a bottom row with stainless steel only

Concrete was cast using cement CEM I N42.5 from a local manufacturer. San was 0/4 mm, while aggregates were 4/10 mm. The water-to-cement ratio was 0.65 to keep the concrete flowable. The compressive strength at 28 days was 23 MPa.

The steel composition is given in **Table 1**. The MS, HC, and SS had chromium contents of 0.013, 9.54, and 18.180, respectively. This is the most significant variance in all the steel types. There are several other elements/constituents are there that are different in each steel type. The yield and tensile strengths of steel were respectively 561 and 664, 937 and 1158, and 609 and 738 for MS, HC, and SS, respectively.

Table 1: Chemical composition of studied steel types

Steel Type	**1. Chemical Composition (%)**													
	C	**Si**	**Mn**	**P**	**S**	**V**	**Nb**	**Cu**	**Ni**	**Cr**	**Mo**	**N**	**CE**	**Co**
MS	0.2	0.14	0.66	0.011	0.014	-	-	0.025	0.021	0.013	-	0.006	0.32	-
SS	0.020	0.290	-	0.0390	0.0240	-	-	0.520	8.010	18.180	0.340	-0.0830	-	0.180
HC	0.1	0.41	0.57	0.011	0.009	0.27	0.019	0.16	0.1	9.54	0.02	0.019	1.15	-

2.1 Conditioning of Block Samples

Samples were conditions under 3.5% NaCl solution. The wetting and drying cycle was applied for two weeks each. The corrosion state was monitored regularly during the testing by open circuit potentials (OPC). Once the OPC falls in a range for mild steel that the corrosion is 100% guaranteed, other electrochemical tests were performed.

2.2 Linear Polarization Resistance/Microcell Current Measurements

Linear polarization resistance (LPR) was applied after corrosion was initiated on each rebar in the block samples. Three electrodes set up were used to obtain the LPR/R_p values. Gamry® 3000 potentiostat was used to perform these experiments. The reference electrode (RE) was the saturated calomel electrode (SCE), while the counter electrode (CE) was titanium mesh. The mesh was placed at the top surface of the concrete block, which is near the top row of reinforcement. RE electrode was placed in the water in which block samples were immersed. A polarization of ± 20 from OCP was applied to rebars to perturb the system and currents were measured.

2.3 Macrocell current

The top rebars after corrosion were connected to the bottom bar to measure the macrocell corrosion current in each type of steel rebar. In this study, the results of only one rebar from the top row connected to a rebar at the bottom row are presented. That is the anode-to-cathode ratio is 1. This will compare the real-time corrosion behavior of steel rebars. Gamry® 3000 potentiostat was used for these experiments. The block samples were kept immersed under water till the top reinforcement row during the experiments. The macrocell between the top and bottom bar was measured until the current become stable.

3 Results and Discussion

3.1 Linear Polarization Resistance (LPR)

The typical results of LPR spectra are shown in Fig. **2**. It can be seen that the range of current range for SS was at least an order lower than the currents observed in the MS and HC. Principally the LPR curves should be straight lines as the polarization increase current should increase linearly around the OCP (Sohail, 2013). However, the LPR curves are slightly crooked at the cathodic polarization side, this is due to the experimental setup of titanium mesh which injects the current that might get astray and results in a slightly nonlinear part in the curve. The Rp values were calculated on the straight/linear portion of the curve.

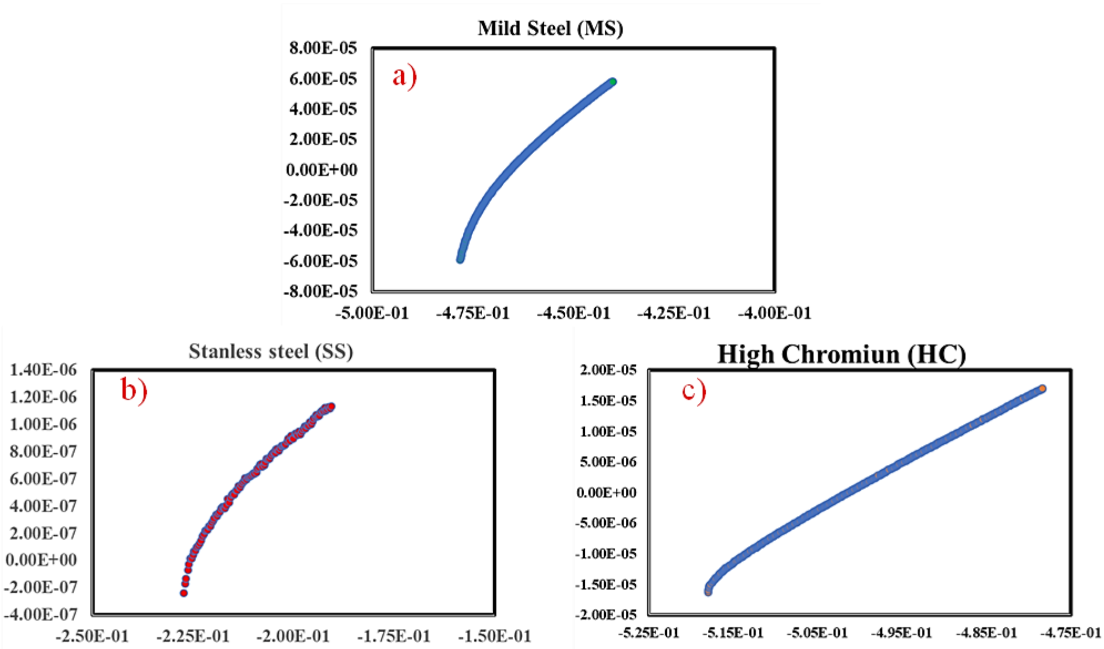

Fig. 2: Linear polarization resistance (LPR) curves. The slope of the LPR curve provides Rp values

The extracted polarization resistance, Rp, is shown in Fig. **3**, for three types of steel rebars. The values were 417, 1294, and 3414 Ohms from MS, HC, and SS, respectively. As the Rp value increases the resistance to corrosion is increased, and vice versa. The polarization resistance is more for SS compared to HC and MS. This is due to a higher amount of chromium in its composition. The HC showed three times higher resistance compared to MS. Sohail et al. (2020) demonstrated that HC has 2-3 times higher corrosion resistance compared to the MS. Which is similar to the results in this study.

Fig. **4** shows the microcell corrosion current extracted from the LPR/Rp values. The values are 62.47, 20.13, and 0.763 µA for MS, HC, and SS respectively. With these values, the corrosion rate is 0.01894, 0.006104, and 0.001143 mm/year respectively for MS, HC, and SS. This shows how fast the rebars will lose their cross-sectional area under active corrosion due to the chloride attack. Losing area will increase the corrosion products in concrete, hence increase the spalling, and cracking in the concrete cover.

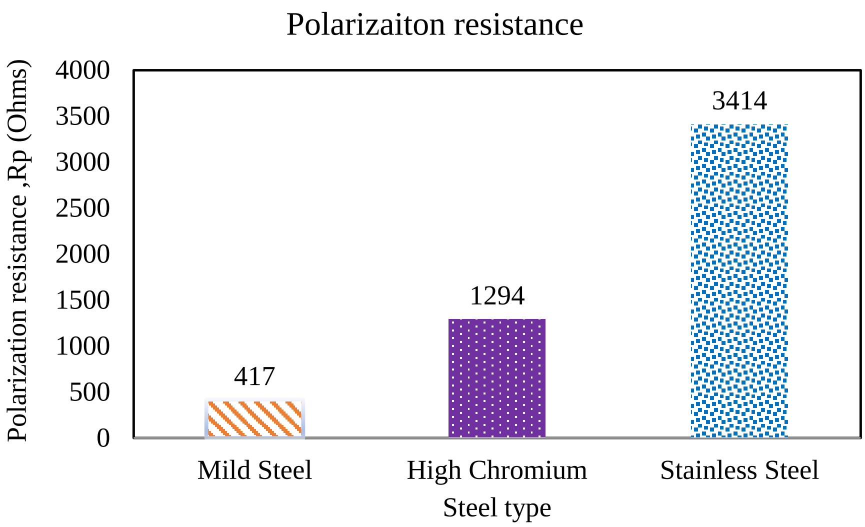

Fig. 3: Polarization resistance of mild steel, high chromium, and stainless steel in the active corrosion state under chloride attack

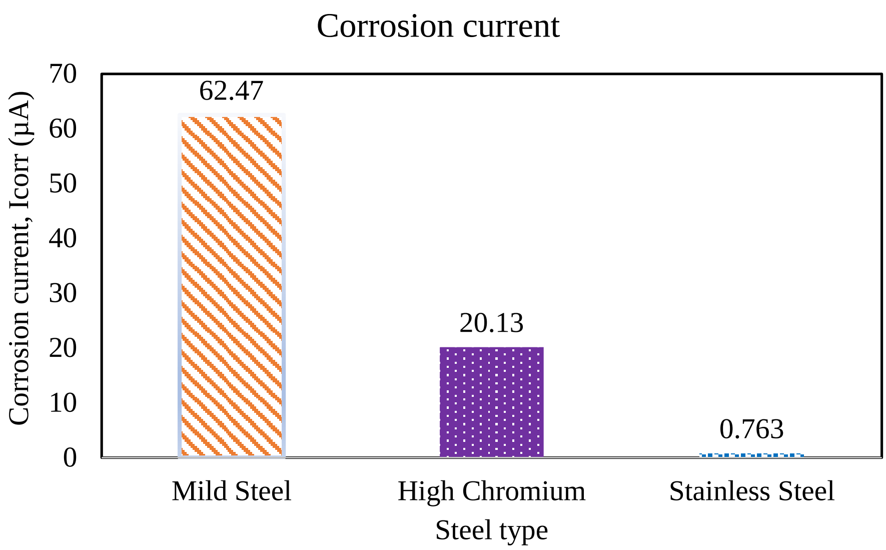

Fig. 4: Microcell corrosion current calculated based on the Rp values in mild steel, high chromium steel, and stainless steel

Fig. 5 presents the macrocell corrosion current in the MS, HC, and SS rebars in the block samples with an A/C ratio of 1. The top bar in the concrete block was connected to the bottom bar directly underneath the top bar. The current was measured until the values are stable between bars.

It is clear that SS performed much better than the other two bars. Its macrocell current was also in nano ampere (nA). Whereas, the macrocell current in the MS and HC was 60 µA and 10 µA, respectively. The macrocell current MS is 6 times higher compared to the HC. Macrocell corrosion causes higher loss in weight and cross-sectional area of steel rebars (Sohail et al., 2015). Hence, the macrocell is more damaging to reinforcement as compared to the microcell corrosion current.

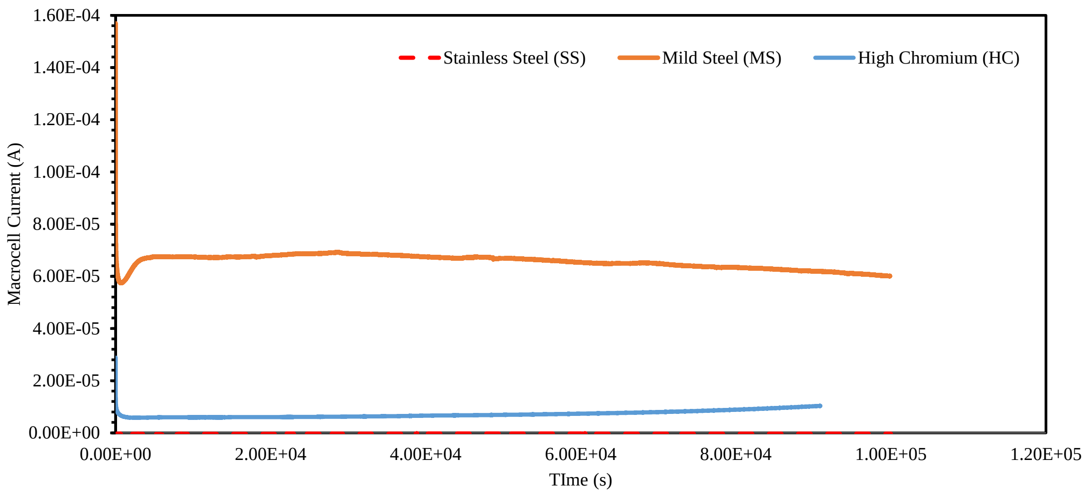

Fig. 5: Macrocell corrosion in block samples with an anode-to-cathode ratio of 1

4 Conclusion

Accelerated corrosion was induced using wetting and drying cycles in the concrete samples reinforced with either mild steel, high chromium steel, or stainless steel rebars. After two years of conditioning, the samples were electrochemically tested with linear polarization resistance, and macrocell current was measured.

Results show that the high chromium steel could be a viable solution as reinforcement where the chloride environment is encountered and corrosion of mild steel is a concern. Stainless steel has performed better than mild and high chromium steel in harsh environments. However, the cost of stainless steel might hinder its use in normal construction. However, for important mega structures subjected to harsh environments, it could be employed to enhance durability.

References

Al Hashem, A. (2011). “Corrosion in Gulf Cooperation Councel (GCC) state: Statistics and figures.” *The Corrosion UAE*, Abu Dhabi, UAE.

Cui, F. & Krauss, P. (2008). *Comparative Corrosion Testing and Analysis of MMFX 2 Rebars for Reinforced Concrete Applications*.

Fahim, et al. (2019). “Corrosion resistance of chromium-steel and stainless steel reinforcement in concrete.” *Materials and Corrosion*, John Wiley & Sons, Ltd, *70*(2), 328–344.

Lim, H. L. (2012). “Assessing Level and Effectiveness of Corrosion Education in the UAE.” *International Journal of Corrosion*, Hindawi, 2012, 1–10.

Mohamed, N., Boulfiza, M. & Evitts, R. (2013). “Corrosion of carbon steel and corrosion-resistant rebars in concrete structures under chloride ion attack.” *Journal of Materials Engineering and Performance*, Springer US, *22*(3), 787–795.

Nachiappan, V. & Cho, E. H. (2005). “Corrosion of High Chromium and Conventional Steels Embedded in Concrete.” *Journal of Performance of Constructed Facilities*, *19*(1), 56–61.

Sohail, M. G. (2013). “Corrosion of steel in concrete: development of an accelerated test by carbonation and galvanic coupling.” PhD Thesis, Universite de Paul Sabatier, Universite de Toulouse III.

Sohail, et al. (2015). “Significance of macrocell corrosion of reinforcing steel in partially carbonated concrete: numerical and experimental investigation.” *Materials and Structures*, *48*(1–2), 217–233.

___. (2019). Corrosion performance of mild steel and epoxy coated rebar in concrete under simulated harsh environment. International Journal of Building Pathology and Adaptation, 37(5), 657–678. https://doi.org/10.1108/IJBPA-12-2018-0099

___. (2018a). “Reinforced Concrete Degradation in the Harsh Climates of the Arabian Gulf: Field Study on 30-to-50-Year-Old Structures.” *Journal of Performance of Constructed Facilities*, American Society of Civil Engineers (ASCE), *32*(5), 04018059 (1–12).

___. (2018b). “Advancements in Concrete Mix Designs: High-Performance and Ultrahigh-Performance Concretes from 1970 to 2016.” *Journal of Materials in Civil Engineering*, *30*(3), 04017310.

___. (2020a). “Electrochemical behavior of mild and corrosion resistant concrete reinforcing steels.” *Construction and Building Materials*, Elsevier Ltd, 232.

___. (2020b). “Durability characteristics of high and ultra-high performance concretes.” *Journal of Building Engineering*, 101669.

___. (2021). “Electrochemical corrosion parameters for active and passive reinforcing steel in carbonated and sound concrete.” *Materials and Corr osion*, John Wiley & Sons, Ltd, 1–18.

___. (2022). “Behavior of artificially corroded RC beams strengthened with CFRP and hybrid CFRP-GFRP laminates.” *Engineering Structures*, Elsevier, *272*, 114827.

Team, P. E. (2007). “Purdue e-Pubs MMFX Microcomposite Steel (MMFX2).”

Cite as: Sohail M.G., Al Nuaimi N., Al-Nahhal W. & Kahraman R., “Performance of Mild Steel and Corrosion-Resistant Steel Rebars in Chloride-Contaminated Concrete”, *The 2nd International Conference on Civil Infrastructure and Construction (CIC 2023)*, Doha, Qatar, 5-8 February 2023, DOI: https://doi.org/10.29117/cic.2023.0103